

Citation

K. Kokilepersaud, M. Prabhushankar, G. AlRegib, S. Trejo Corona, C. Wykoff "Gradient-Based Severity Labeling for Biomarker Classification in OCT," in *2022 IEEE International Conference on Image Processing (ICIP), Bordeaux, France, 2022*.

Review

Date of Acceptance: June 6th 2022

Codes

https://github.com/olivesgatech/Severity_Contrastive_Learning.git

Bib

```
@inproceedings{kokilepersaud2022severity,  
title={Gradient-Based Severity Labeling for Biomarker Classification in OCT},  
author={Kokilepersaud, Kiran and Prabhushankar, Mohit and AlRegib, Ghassan and Trejo  
Corona, Stephanie and Wykoff, Charles},  
booktitle={IEEE International Conference on Image Processing},  
year={2022}}
```

Contact

{kpk6, mohit.p, alregib}@gatech.edu
<https://ghassanalregib.info/>

**Corresponding
Author**

alregib@gatech.edu

GRADIENT-BASED SEVERITY LABELING FOR BIOMARKER CLASSIFICATION IN OCT

Kiran Kokilepersaud* Mohit Prabhushankar* Ghassan AlRegib* Stephanie Trejo Corona† Charles Wykoff†

* OLIVES at the Center for Signal and Information Processing CSIP,
School of Electrical and Computer Engineering, Georgia Institute of Technology, Atlanta, GA, USA

† Retina Consultants Texas, Retina Consultants of America, Houston, Texas, USA
{kpk6, mohit.p, alregib}@gatech.edu {stephanie.trejo, ccwmd}@retinaconsultantstexas.com

ABSTRACT

In this paper, we propose a novel selection strategy for contrastive learning for medical images. On natural images, contrastive learning uses augmentations to select positive and negative pairs for the contrastive loss. However, in the medical domain, arbitrary augmentations have the potential to distort small localized regions that contain the biomarkers we are interested in detecting. A more intuitive approach is to select samples with similar disease severity characteristics, since these samples are more likely to have similar structures related to the progression of a disease. To enable this, we introduce a method that generates disease severity labels for unlabeled OCT scans on the basis of gradient responses from an anomaly detection algorithm. These labels are used to train a supervised contrastive learning setup to improve biomarker classification accuracy by as much as 6% above self-supervised baselines for key indicators of Diabetic Retinopathy.

Index Terms— Retinal Biomarkers, Contrastive Learning, Gradients

1. INTRODUCTION

Diabetic Retinopathy (DR) is the leading cause of irreversible blindness among people aged 20 to 74 years old [1]. In order to manage and treat DR, the detection and evaluation of biomarkers of the disease is a necessary step for any clinical practice [2]. Biomarkers refer to “any substance, structure, or process that can be measured in the body or its products and influence or predict the incidence of outcome or disease [3].” Biomarkers such as those in Figure 1 are important indicators of DR and give ophthalmologists a fine-grained understanding of the manifestation of DR for individual patients.

Due to the importance of biomarkers in the clinical decision making process, much work has gone into deep learning methods to automate their detection directly from optical coherence tomography (OCT) scans [4]. A major bottleneck hindering this goal is the dependence of conventional deep learning architectures on having access to a large training pool. This dependency is not generalizable to the medical domain where biomarker labels are expensive to curate,

due to the requirement of expert graders. In order to move beyond this limitation, contrastive learning [5] has been one of the research directions to leverage the larger set of unlabeled data to improve performance on the smaller set of labeled data. Contrastive learning approaches operate by creating a representation space through minimizing the distance between positive pairs of images and maximizing the distance between negative pairs. Traditional approaches like [6] generate positive pairs from taking augmentations from a single image and treating all other images in the batch as the negative pairs. This makes sense from a natural image perspective, but from a medical point of view the augmentations utilized in these strategies, such as gaussian blurring, can potentially distort small localized regions that contain the biomarkers of interest. Examples of regions that could potentially be occluded are indicated by white arrows in Figure 1. A more intuitive approach from a medical perspective would be to select positive pairs that are at a similar level of *severity*. Images with similar disease severity levels share structural features in common that manifest itself during the progression of DR [7]. Hence, choosing positive pairs on the basis of severity can better bring together OCT scans with similar structural components in a contrastive loss. It is also possible to view more severe samples as existing on a separate manifold from the healthy trained images as shown in Figure 2. From this manifold outlook of severity, some model response can be calculated as a severity score that indicates how far a sample is from the healthy manifold. To capture this intuition, we introduce the description of severity as “the degree to which a sample appears anomalous relative to the distribution of healthy images.” From this perspective, one way to measure severity is by formulating it as an anomaly detection problem where some response from a trained network can serve to identify the degree to which a sample differs from healthy images through a severity score.

We argue in this work that the appropriate model response to measure is the gradient from the update of a model. Gradients represent the model update required to incorporate new data. From this intuition, gradients have been shown to be able to represent the learned representation

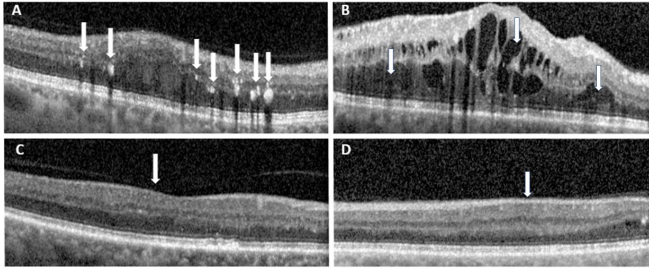


Fig. 1: OCT Scans of biomarkers from the Prime + TREX DME datasets. The biomarkers are A) Intraretinal Hyperreflective Foci (IRHRF), B) Intraretinal Fluid (IRF) and Diabetic Macular Edema (DME) C) Partially Attached Vitreous Face (PAVF), and D) Fully Attached Vitreous Face (FAVF). The white arrows point out examples of where these biomarkers are found in the images. A discussion of biomarkers in OCT can be found at [2].

space from a model [8], represent contrastive explanations between classes [9], and perform contrastive reasoning [10]. Anomalous samples require a more drastic update to be represented than normal samples [11]. Additionally, previous work [12] showed that gradient information could be used to effectively rank samples into subsets that exhibit semantic similarities. Hence, in this work, we propose to use gradient measures from an anomaly detection methodology known as GradCON [13] to assign pseudo severity labels to a large set of unlabeled OCT scans. We utilize these severity labels to train an encoder with a supervised contrastive loss [14] and then fine-tune the representations learnt on a smaller set of available biomarker labels. In this way, we leverage a larger set of easy to obtain healthy images and unlabeled data to improve performance in a biomarker classification task. The contributions of this paper are: **1)** We propose a framework to assign severity pseudo-labels to unlabeled OCT scans on the basis of gradient responses. **2)** We show the effectiveness of these weak severity labels in a contrastive learning framework to improve biomarker classification performance.

2. RELATION TO PRIOR WORK

Self-Supervised learning for OCT images: Traditional deep learning approaches for OCT have relied on access to a large quantity of labeled data. For example, [4] showed how transfer learning could be applied to learn classification of retinal disease indicators. Similarly, [15] introduced a transfer learning scheme to detect pupillary defects. Methods like this demonstrate the capability of deep learning in OCT, but their dependence on potentially expensive labels makes them sub-optimal for the various constraints of the medical field. This has motivated self-supervised strategies such as [16] where a model was trained to learn the time interval between patient visits for characterizing disease progression in OCT. [17] also used patient information as well as modality-

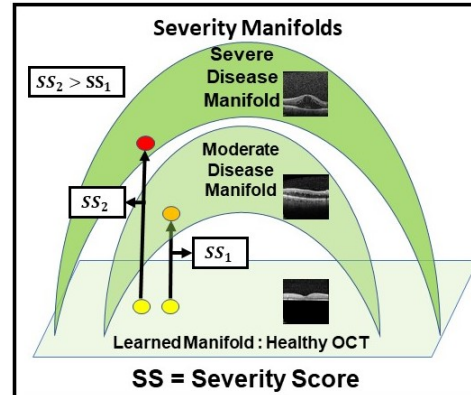


Fig. 2: From a healthy manifold learned from a trained auto-encoder, we can compute distance to the manifold of more severely diseased cases via a Severity Score (SS). Severity Score is calculated via some model response and increases as a sample is more anomalous compared to the learned healthy manifold.

invariant features to detect Age-related macular degeneration (AMD). [18] crated a dual framework leveraging labeled and unlabeled data for anomaly detection tasks in OCT scans. These works introduce self-supervised ideas to OCT, but differs from ours from the perspective of our pseudo-labeling process and the usage of a supervised contrastive loss.

Contrastive Learning in Medical domain: Previous work has shown that traditional contrastive learning approaches such as [5] and [6] work within the medical domain [19]. However, improvements have been sought by identifying more informed ways to choose positive instances. [20] showed how choosing positive instances from the same patient can improve classification of Chest X-ray scans. Similarly, [21] utilized a subject-aware contrastive learning with brain wave signals for the task of anomaly detection. [22] used a supervised contrastive loss based on position within a volume. Each of these works are similar to ours in that they seek to introduce a medically consistent way to choose positive pairs from data for a contrastive loss. However, our work differs because it introduces a new methodology for choosing positive pairs of data based on weak disease severity labeling.

3. METHODOLOGY

3.1. Datasets

The two datasets of interest are the healthy images from the Kermany dataset [23] and Prime + TREX DME [24, 25]. We will refer to these datasets as the “Healthy” dataset and the “Biomarker” dataset respectively. The training set of the Biomarker dataset consists of approximately 60000 unlabeled OCT scans and 7500 OCT scans with explicit biomarker labels from 76 different eyes. These OCT scans were collected

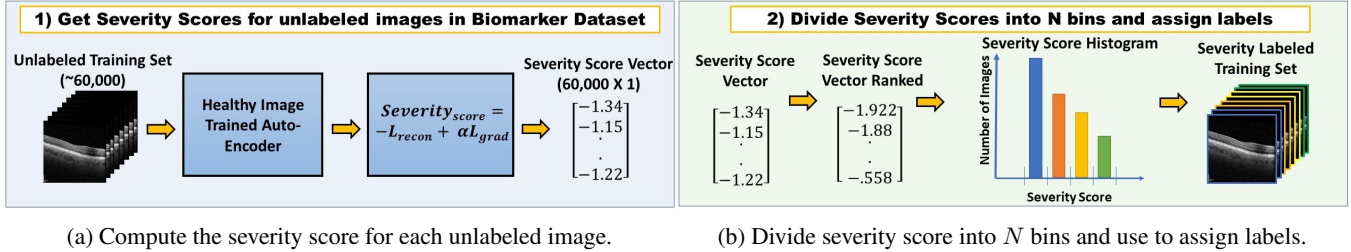


Fig. 3: Overview of severity labeling methodology.

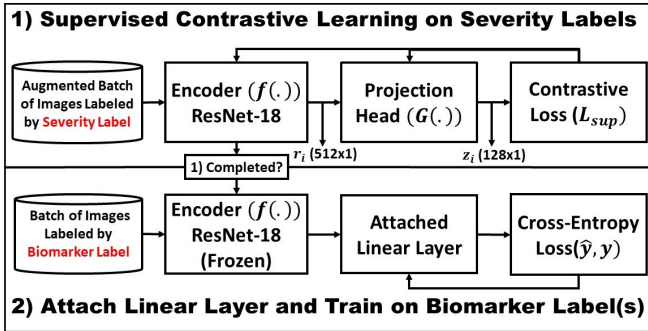


Fig. 4: Overview of supervised contrastive learning and linear fine-tuning steps. 1) Supervised Contrastive Loss on generated severity labels from previously unlabeled data. 2) Attach linear layer and train on labeled biomarker data.

as part of the Prime and TREX DME studies at the Retina Consultants of Texas (RCTX). For each labeled OCT scan in the Biomarker dataset, a trained grader performed interpretation on OCT scans for the presence or absence of 20 different biomarkers. Among these biomarkers, 5 exist in balanced quantities to be used in training for the binary classification task of detecting the biomarker of interest. These biomarkers include those found in figure 1. OCT scans from 76 eyes constitute the training set and the OCT scans from a remaining set of 20 eyes make up the test set. From these test OCT scans, random sampling was employed to develop an individualized test set for each of the 5 biomarkers used in our analysis. This resulted in a balanced test set, for each biomarker, where 500 OCT Scans have the biomarker present and 500 OCT Scans have the biomarker absent.

3.2. Severity Label Generation

The first step in our methodology is to learn the distribution of healthy OCT scans. To do this, the images from the Healthy dataset are resized to 224×224 and used to train an auto-encoder through the GradCON methodology introduced by [13]. The intuition behind this work is to introduce a gradient constraint during training so that gradients from healthy images will align more closely together. This encourages images that deviate from the healthy distribution to have

gradients that are more distinguishable. Once we have this trained auto-encoder, we follow the methodology detailed in Figure 3. The first step is to get the severity score for all unlabeled images in the Biomarker dataset. To do this, we pass all unlabeled images to the input of the trained auto-encoder network and extract their corresponding severity score that is represented by equation 1.

$$\text{Severity Score (SS)} = -L_{recon} + \alpha L_{grad} \quad (1)$$

L_{recon} is the mean squared error between an input x and its reconstructed output \hat{x} . L_{grad} is the average of the cosine similarity between the gradients of the target image and the reference gradients learned from training on the healthy dataset across all layers of the decoder. α was set to .03 for all experiments. This results in every image having an associated severity score which constitutes a severity score vector. Once we have this severity score vector, we move to step 2 in Figure 3, where the severity labels for each image are generated. This is done by ranking the severity scores in ascending order. These ranked scores are then divided into N bins based on having a similar severity score to other images. Images belonging to the same severity score bin are given the same severity label (SL) for use in the next stage of our setup. This results in the previously unlabeled data now having one of N possible labels. Note that N is a hyper-parameter that is explored experimentally in this paper. To get an intuitive sense of the quality of these severity labels we sample images randomly from the bins at the extreme ends of the histogram and end up with Figure 5. It can be observed that the lower severity scores correspond with images that are healthier than those at the other end of the distribution. This makes sense as lower severity scores indicate that the image's gradients have a greater alignment with the gradients of the learned healthy distribution.

3.3. Supervised Contrastive Loss on Severity Labels

Once we have the severity labels (SL), we utilize the supervised contrastive loss [14] to bring embeddings of images with the same label together and push apart embeddings of images with differing labels. The overall setup is detailed through the flowchart shown in Figure 4. The first step described is how the training of the encoder with the supervised

contrastive loss progresses. Each image x_i is passed through an encoder network $f(\cdot)$, that we set to be ResNet-18 [26], producing a 512×1 dimensional vector r_i . This vector is further compressed through a projection head $G(\cdot)$ which is set to be a multi-layer perceptron with a single hidden layer. This projection head is used to reduce the dimensionality of the representation and is discarded after training. The output of $G(\cdot)$ is a 128×1 dimensional embedding z_i . In this embedding space, the dot product of images with the same severity label (the positive samples) are maximized and those with different severity labels (the negative samples) are minimized. This takes the form of equation 2 where positive instances for image x_i come from the set $P(i)$ and positive and negative instances come from the set $A(i)$. τ is a temperature scaling parameter set to .07 for all experiments. z_p refers to the embeddings of the set of positive instances and z_a indicates embeddings of all positive and negative instances.

$$L_{sup} = \sum_{i \in I} \frac{-1}{|P(i)|} \sum_{p \in P(i)} \log \frac{\exp(z_i \cdot z_p / \tau)}{\sum_{a \in A(i)} \exp(z_i \cdot z_a / \tau)} \quad (2)$$

After training the encoder, we move to step 2 of the methodology described in Figure 4 where the model explicitly learns to detect biomarkers. To do this, the weights of the encoder are frozen and a linear layer is appended to the output of the encoder. We utilize the subset of the Biomarker dataset with biomarker labels for fine-tuning on top of the representation space learnt in step 1 of Figure 4. A biomarker is chosen to be the one we are interested in and a linear layer is trained using cross-entropy loss between a predicted output \hat{y} and a ground truth label y to learn to detect the presence or absence of the biomarker in the image.

4. EXPERIMENTS

The proposed strategy is compared against three state of the art self-supervised strategies that make use of the unlabeled data. The architecture was kept constant as ResNet-18 across all experiments. Augmentations included random resize crop to a size of 224, horizontal flip, color jitter, and normalization to the mean and standard deviation of the respective dataset. The batch size was set at 64. Training was performed for 25 epochs in every setting. A stochastic gradient descent optimizer was used with a learning rate of $1e-3$ and momentum of .9. Accuracy and F1-score was recorded for the testing of performance on each individual biomarker. Additionally, we assess the method’s capability across all biomarkers by utilizing a mean AUC metric within a multi-label classification setting for the labels of all 5 biomarkers at the same time.

Overall, choosing of the severity bin hyperparameter N has significant influence on performance improvements on both multi-label classification performance as well as detection performance on individual biomarkers. Table 1 represents the complete results for this study. SL_N represents

the encoder trained after dividing the unlabeled pool into N severity label bins. This is repeated for different number of severity bin divisions ranging from 5000 to 20000. A larger number of bins means the images within each bin are more likely to share structures in common, but at the trade-off of having fewer positive instances during training. A more moderate choice for number of severity bins, such as 5000 or 10000, led to improved performance in multi-class classification compared to all baselines. However, it was also observed that choosing larger or smaller values for the number of bins resulted in best performance for specific biomarkers. For example, the best performing values for DME and IRF resulted at the higher number of severity bins of 15000 and 20000. Additionally, the best result for PAVF was at a severity bin value of 10000. The variation in performance for different bin numbers can also be understood from the perspective of how fine-grained individual biomarkers are. IRF and DME manifest themselves more distinctively than IRHRF, FAVF, or PAVF. Therefore, it’s possible that a lower number of more closely related positives may be better for identifying these distinctive features. However, in the case of more difficult to identify biomarkers, it may be the case that some level of diversity in the positives is necessary to identify them from the surrounding structures in the OCT scan.

We also studied the effect of using other anomaly detection methods to generate severity scores. We trained a classifier using the labeled data from the Biomarker dataset. Using the output logits from this classifier, we can generate anomaly scores for each the methods shown in Table 2. These scores are then processed in the same way as Figure 3 to generate labels for the unlabeled dataset. These labels are used in the same way as the methodology introduced in this paper to train an encoder with a supervised contrastive loss. Performance is measured by the average AUC value from a multi-label classification setting. We observe that our method with the same level of discretization out-performs all other anomaly detection methodologies.

5. CONCLUSION

Contrastive learning is useful to the medical domain because it allows us to integrate a large pool of unlabeled data into the training process. It relies on methods of choosing good positive and negative pairs of images. We show in this paper that one such approach is to choose pairs based on how anomalous they appear relative to a learned healthy class distribution. We show that defining this degree of abnormality through a gradient response leads to semantically interpretable clusters under a common label that can be used within a supervised contrastive learning framework. Training on these labels leads to an improved representation space that out-performs state of the art self-supervised methods.

Severity Label Training Results (Accuracy / F1-Score)						
Method	IRF	DME	IRHRF	FAVF	PAVF	Multi-Label
SimCLR [6]	75.13% / .715	80.61% / .772	59.03% / .675	75.43% / .761	52.69% / .249	.754
PCL [27]	76.50% / .717	80.11% / .761	59.1% / .683	76.30% / .773	51.40% / .165	.767
Moco v2 [5]	76.00% / .720	82.24% / .793	59.6% / .692	75.00% / .784	52.5% / .201	.769
SL_{5000}	75.20% / .698	81.46% / .786	66.83% / .695	75.39% / .756	54.7% / .314	.774
SL_{10000}	75.46% / .732	82.35% / .796	62.00% / .700	73.56% / .722	56.69% / .370	.771
SL_{15000}	74.33% / .701	84.52% / .831	59.86% / .691	72.03% / .726	55.56% / .322	.765
SL_{20000}	76.13% / .733	81.12% / .788	62.93% / .703	71.90% / .745	54.03% / .258	.766

Table 1: Performance of severity labeling and supervised contrastive learning approach on individual biomarkers. Multi-Label is the average AUC from the multi-label classification task. SL_N refers to training an encoder after having divided the training set into N severity label bins.

Anomaly Detector Ablation Study	
Method	Multi-Label
MSP [28]	.764
ODIN [29]	.761
Mahalabonis [30]	.772
SL	.774

Table 2: Analysis of using different anomaly detectors to generate severity labels. For each method scores were generated for each unlabeled image in the Biomarker dataset and discretized into 5000 bins.

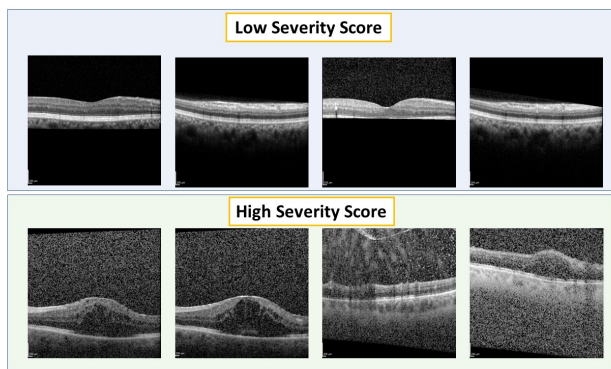


Fig. 5: Visual representation of OCT scans with high and low severity scores.

6. REFERENCES

- [1] Donald S Fong, Lloyd Aiello, Thomas W Gardner, George L King, George Blankenship, Jerry D Cavallerano, Fredrick L Ferris III, Ronald Klein, and American Diabetes Association, “Retinopathy in diabetes,” *Diabetes care*, vol. 27, no. suppl_1, pp. s84–s87, 2004.
- [2] Ashish Markan, Aniruddha Agarwal, Atul Arora, Krinjeela Bazgain, Vipin Rana, and Vishali Gupta, “Novel imaging biomarkers in diabetic retinopathy and diabetic macular edema,” *Therapeutic Advances in Ophthalmology*, vol. 12, pp. 2515841420950513, 2020.
- [3] Kyle Strimbu and Jorge A Tavel, “What are biomarkers?,” *Current Opinion in HIV and AIDS*, vol. 5, no. 6, pp. 463, 2010.
- [4] Daniel S Kermany, Michael Goldbaum, Wenjia Cai, Carolina CS Valentim, Huiying Liang, Sally L Baxter, Alex McKeown, Ge Yang, Xiaokang Wu, Fangbing Yan, et al., “Identifying medical diagnoses and treatable diseases by image-based deep learning,” *Cell*, vol. 172, no. 5, pp. 1122–1131, 2018.
- [5] Xinlei Chen, Haoqi Fan, Ross Girshick, and Kaiming He, “Improved baselines with momentum contrastive learning,” *arXiv preprint arXiv:2003.04297*, 2020.
- [6] Ting Chen, Simon Kornblith, Mohammad Norouzi, and Geoffrey Hinton, “A simple framework for contrastive learning of visual representations,” in *International conference on machine learning*. PMLR, 2020, pp. 1597–1607.
- [7] Xiaogang Wang, Yongqing Han, Gang Sun, Fang Yang, Wen Liu, Jing Luo, Xing Cao, Pengyi Yin, Frank L Myers, and Liang Zhou, “Detection of the microvascular changes of diabetic retinopathy progression using optical coherence tomography angiography,” *Translational Vision Science & Technology*, vol. 10, no. 7, pp. 31–31, 2021.
- [8] Gukyeong Kwon, Mohit Prabhushankar, Dogancan Temel, and Ghassan AlRegib, “Distorted representation space characterization through backpropagated gradients,” in *2019 IEEE International Conference on Image Processing (ICIP)*. IEEE, 2019, pp. 2651–2655.
- [9] Mohit Prabhushankar, Gukyeong Kwon, Dogancan Temel, and Ghassan AlRegib, “Contrastive explanations in neural networks,” in *2020 IEEE International Conference on Image Processing (ICIP)*. IEEE, 2020, pp. 3289–3293.

- [10] Mohit Prabhushankar and Ghassan AlRegib, “Contrastive reasoning in neural networks,” *arXiv preprint arXiv:2103.12329*, 2021.
- [11] Jinsol Lee and Ghassan AlRegib, “Gradients as a measure of uncertainty in neural networks,” in *2020 IEEE International Conference on Image Processing (ICIP)*. IEEE, 2020, pp. 2416–2420.
- [12] Chirag Agarwal, Daniel D’souza, and Sara Hooker, “Estimating example difficulty using variance of gradients,” *arXiv preprint arXiv:2008.11600*, 2020.
- [13] Gukyeong Kwon, Mohit Prabhushankar, Dogancan Temel, and Ghassan AlRegib, “Backpropagated gradient representations for anomaly detection,” in *European Conference on Computer Vision*. Springer, 2020, pp. 206–226.
- [14] Prannay Khosla, Piotr Teterwak, Chen Wang, Aaron Sarna, Yonglong Tian, Phillip Isola, Aaron Maschinot, Ce Liu, and Dilip Krishnan, “Supervised contrastive learning,” *arXiv preprint arXiv:2004.11362*, 2020.
- [15] Dogancan Temel, Melvin J Mathew, Ghassan AlRegib, and Yousuf M Khalifa, “Relative afferent pupillary defect screening through transfer learning,” *IEEE Journal of Biomedical and Health Informatics*, vol. 24, no. 3, pp. 788–795, 2019.
- [16] Antoine Rivail, Ursula Schmidt-Erfurth, Wolf-Dieter Vogl, Sebastian M Waldstein, Sophie Riedl, Christoph Grechenig, Zhichao Wu, and Hrvoje Bogunovic, “Modeling disease progression in retinal octs with longitudinal self-supervised learning,” in *International Workshop on Predictive Intelligence In Medicine*. Springer, 2019, pp. 44–52.
- [17] Xiaomeng Li, Mengyu Jia, Md Tauhidul Islam, Lequan Yu, and Lei Xing, “Self-supervised feature learning via exploiting multi-modal data for retinal disease diagnosis,” *IEEE Transactions on Medical Imaging*, vol. 39, no. 12, pp. 4023–4033, 2020.
- [18] Yuhan Zhang, Mingchao Li, Zexuan Ji, Wen Fan, Songtao Yuan, Qinghuai Liu, and Qiang Chen, “Twin self-supervision based semi-supervised learning (ts-ssl): Retinal anomaly classification in sd-oct images,” *Neurocomputing*, 2021.
- [19] Hari Sowrirajan, Jingbo Yang, Andrew Y Ng, and Pranav Rajpurkar, “Moco-cxr: Moco pretraining improves representation and transferability of chest x-ray models,” *arXiv preprint arXiv:2010.05352*, 2020.
- [20] Yen Nhi Truong Vu, Richard Wang, Niranjan Balachandar, Can Liu, Andrew Y Ng, and Pranav Rajpurkar, “Medaug: Contrastive learning leveraging patient metadata improves representations for chest x-ray interpretation,” *arXiv preprint arXiv:2102.10663*, 2021.
- [21] Joseph Y Cheng, Hanlin Goh, Kaan Dogrusoz, Oncel Tuzel, and Erdrin Azemi, “Subject-aware contrastive learning for biosignals,” *arXiv preprint arXiv:2007.04871*, 2020.
- [22] Dewen Zeng, Yawen Wu, Xinrong Hu, Xiaowei Xu, Haiyun Yuan, Meiping Huang, Jian Zhuang, Jingtong Hu, and Yiyu Shi, “Positional contrastive learning for volumetric medical image segmentation,” *arXiv preprint arXiv:2106.09157*, 2021.
- [23] Daniel Kermany, Kang Zhang, and Michael Goldbaum, “Large dataset of labeled optical coherence tomography (oct) and chest x-ray images,” *Mendeley Data*, vol. 3, pp. 10–17632, 2018.
- [24] John F Payne, Charles C Wykoff, W Lloyd Clark, Beau B Bruce, David S Boyer, and David M Brown, “Long-term outcomes of treat-and-extend ranibizumab with and without navigated laser for diabetic macular oedema: Trex-dme 3-year results,” *British Journal of Ophthalmology*, vol. 105, no. 2, pp. 253–257, 2021.
- [25] J Yu Hannah, Justis P Ehlers, Duriye Damla Sevgi, Jenna Hach, Margaret O’Connell, Jamie L Reese, Sunil K Srivastava, and Charles C Wykoff, “Real-time photographic-and fluorescein angiographic-guided management of diabetic retinopathy: Randomized prime trial outcomes,” *American Journal of Ophthalmology*, vol. 226, pp. 126–136, 2021.
- [26] Kaiming He, Xiangyu Zhang, Shaoqing Ren, and Jian Sun, “Deep residual learning for image recognition,” in *Proceedings of the IEEE conference on computer vision and pattern recognition*, 2016, pp. 770–778.
- [27] Junnan Li, Pan Zhou, Caiming Xiong, and Steven CH Hoi, “Prototypical contrastive learning of unsupervised representations,” *arXiv preprint arXiv:2005.04966*, 2020.
- [28] Dan Hendrycks and Kevin Gimpel, “A baseline for detecting misclassified and out-of-distribution examples in neural networks,” *arXiv preprint arXiv:1610.02136*, 2016.
- [29] Shiyu Liang, Yixuan Li, and Rayadurgam Srikant, “Enhancing the reliability of out-of-distribution image detection in neural networks,” *arXiv preprint arXiv:1706.02690*, 2017.
- [30] Kimin Lee, Kibok Lee, Honglak Lee, and Jinwoo Shin, “A simple unified framework for detecting out-of-distribution samples and adversarial attacks,” *Advances in neural information processing systems*, vol. 31, 2018.